On the Generation of Broad-Band Beams for a Nondispersive Time-Signal Transmission

Itsik Dvir and Pinchas D. Einziger

***Abstract*— A novel aperture synthesis method is proposed for a broad-band beam (BB) generation, which supports a nondispersive time-signal transmission to a single observation plane. This plane, regarded here as the image plane (IP), is perpendicular to the axis of propagation and its location can be varied continuously from the near-field zone to the far-field zone. The spatial field of the BB at the IP can be shaped by modifying the classical spatial filtering synthesis techniques to construct a predetermined localized space–time (ST) field. The method characteristics, effectiveness, and simplicity, are demonstrated through two opposing analytic examples: Gaussian and rectangular source-field-distributions (SFD's).**

***Index Terms*— Beams, broad-band beams, electromagnetic pulse, electromagnetic transient propagation, Gaussian beams, nondispersive time signal transmission, pulse generation.**

I. Introduction

PULSED beams characterized by highly localized electromagnetic energy in space–time (ST), have received due attention recently [1]–[4]. The localization property is most promising in applications such as ultrawide bandwidth pulse-driven arrays, covert broad-band communication, and high-resolution detection and reconstruction of objects. In some of these applications, the time envelope of the pulsed beam has to be maintained undistorted. Unfortunately, strong distortion is unavoidable due to the ST dispersion associated with the propagation mechanism of the broad-band time signal, even in homogenous nondispersive media. The objective of this work is to overcome the distortion problem by properly synthesizing the ST source-field distribution (SFD) to obtain an undistorted time envelope at all prescribed observation points.

Synthesis of source functions of array elements for pulse radiation in the far-field zone have been considered by using numerical approaches to achieve optimum performance under specific criteria [5]–[7]. Specifically, optimization problems have been studied to maximize; at a far-field point, the electric field amplitude of the transient radiated field at a specific time [5] or the radiated energy in a specified time interval [6], where constraints have been imposed on the total energy and the frequency bandwidth of the input signals at the terminals of a linear dipole array. A least-square inverse propagating approach have been proposed [7] to find the corresponding driving functions of a given array of radiating elements when a scalar representation of a desired propagating field is given at a finite number of remote spatial locations. An optimum set of the unknown array driving functions has been calculated by solving a system of linear equations in the frequency domain for each frequency component.

This paper addresses a different inverse propagating problem [8]–[10], namely how to synthesize the broad-band beam (BB) aperture field for a nondispersive transmission of a time signal to all observation points located at the image plane (IP).

We solve this problem analytically through a closed-form inversion of the radiation integral associated with paraxial (beam-type) fields. An explicit expression for the BB SFD is formulated in terms of a time-harmonic SFD specified at some typical frequency. Each type of BB corresponds to a unique time-harmonic SFD and can be synthesized by modifying the classical spatial filtering techniques [11].

In contrast to the above previously published numerical optimization schemes, the proposed method has three distinct features: 1) a *unique closed-form* solution; 2) the solution is valid in the *near-field zone* as well; and 3) the solution depends *continuously* on the ST variables, thus it may be implemented by array elements through an appropriate discretization.

The paper is organized as follows. In Section II, the BB integral representation is formulated for nondispersive transmission of signals. In Section III, we present the main result, an explicit expression for the synthesized BB SFD. Sections IV and V introduce closed-form expressions and numerical results, respectively, derived for the Gaussian and rectangular BB SFD's. A summary and general conclusions of this work are given in Section VI.

II. The BB Integral Representation

Let an aperture, located at the $z = 0$ plane in a Cartesian coordinate system, be driven everywhere with a broad-band signal $s(t)$, which is known by its spectral content $s(\omega) \triangleq \int_{-\infty}^{\infty} dt\, s(t) \exp(i\omega t)$. Then, using the well-known aperture theory formulations, the transient fields can be represented as follows [12]:

$$s(\omega)\mathbf{e_t}(\mathbf{r}', \omega) \tag{1}$$

$$s(\omega)\mathbf{E_t}(\mathbf{r}, \omega) \tag{2}$$

where $\mathbf{e_t}(\mathbf{r}', \omega)$ and $\mathbf{E_t}(\mathbf{r}, \omega)$ are the time-harmonic tangential electric vectors at the source plane $\mathbf{r}' \triangleq (x', y', 0)$ and the observation point $\mathbf{r} \triangleq (x, y, z)$, respectively. The half-space

Manuscript received December 30, 1994; revised April 13, 1996.

I. Dvir was with the Department of Electrical Engineering, Technion, Israel Institute of Technology, Haifa, 32000, Israel. He is now with RAFAEL, Haifa, 31021 Israel.

P. D. Einziger is with the Department of Electrical Engineering, Technion, Israel Institute of Technology, Haifa, 32000 Israel.

Publisher Item Identifier S 0018-926X(98)09680-X.

$z > 0$ is assumed to be linear, homogenous, dispersionless, lossless, and isotropic medium.

Next, referring to $\mathbf{E_t}(\mathbf{r}, \omega)$ in (2) as the system transfer function, we impose the following well-known necessary and sufficient constraint:

$$\mathbf{E_t}(\mathbf{r_o}, \omega) = \mathbf{E_t}(\mathbf{r_o}, \omega_0) \exp[i(\omega - \omega_0)\tau(\mathbf{r_o})] \tag{3}$$

which guarantees a nondispersive signal transmission to the prescribed observation point set, $\mathbf{r_o} \triangleq (x_o, y_o, z_o)$. Namely, $\mathbf{E_t}(\mathbf{r_o}, \omega)$ is represented as a product of a frequency-independent attenuation and a linear phase-shift term. The parameter $\tau(\mathbf{r_o})$ in (3) is a time-delay constant related to the traveling time to $\mathbf{r_o}$ and ω_0 is a typical frequency, which can be arbitrarily selected. The left-hand side (LHS) of (3) $\mathbf{E_t}(\mathbf{r_o}, \omega)$ can be written explicitly using spatial convolution formulation [13], [14], known as the Rayleigh–Sommerfeld integral [15]

$$-\frac{1}{2\pi}\frac{\partial}{\partial z}\int \mathbf{dr'}\, \mathbf{e_t}(\mathbf{r'}, \omega)\frac{\exp(i\omega R_o/c)}{R_o} = \mathbf{E_t}(\mathbf{r_o}, \omega_0) \exp[i(\omega - \omega_0)\tau(\mathbf{r_o})] \tag{4}$$

which constitutes an integral relation between the unknown field $\mathbf{e_t}(\mathbf{r'}, \omega)$ and $\mathbf{E_t}(\mathbf{r_o}, \omega_0)$. In (4), $R_o \triangleq [(x_o - x')^2 + (y_o - y')^2 + z_o^2]^{1/2}$ is the distance from $\mathbf{r'}$ to $\mathbf{r_o}$, c is the velocity, and $\mathbf{dr'} \triangleq dx'dy'$ represents two-dimensional (2-D) integration variables.

Since propagation of a beam wave is localized around the beam axis, the parabolic approximation [15]–[20] can be applied to reduce (4) into a simpler form

$$\frac{\omega}{2\pi i c z_o}\int \mathbf{dr'}\, \mathbf{e_t}(\mathbf{r'}, \omega) \exp\left[i\frac{\omega}{c}\left(\frac{r'^2}{2z_o} - \frac{\mathbf{r_o}\cdot\mathbf{r'}}{z_o}\right)\right] = \mathbf{E_t}(\mathbf{r_o}, \omega_0) \exp[-i\omega_0\tau_p(\mathbf{r_o})] \tag{5}$$

i.e., a Fresnel convolution integral. Here, the undetermined time-delay $\tau(\mathbf{r_o})$ in (3) assumes an explicit form

$$\tau_p(\mathbf{r}) \triangleq \frac{\tilde{r}}{c} \tag{6}$$

where

$$\tilde{r} \triangleq z + \frac{x^2 + y^2}{2z} \tag{7}$$

is the parabolic approximation of the observation distance. It is well recognized that the accuracy of the Fresnel approximation is extremely good throughout the far-field and near-field zones for observation points in the beam [15], [20].

In general, a complete inversion of (4), which must be carried out for all frequencies [one-dimensional (1-D) space] and for all $\mathbf{r_o}$ points [three-dimensional (3-D) space], may become quite cumbersome task. Furthermore, uniqueness and existence of the solution are open problems, which seems to be strongly dependent on the selection of both $\mathbf{E_t}(\mathbf{r_o}, \omega_0)$ and the observation point set. However, recognizing $\mathbf{E_t}(\mathbf{r_o}, \omega)$ in (3) as the geometrical optics field [21], we may conclude that nondispersive signals indeed propagate along the set of the geometrical optics rays and that $\mathbf{e_t}(\mathbf{r'}, \omega)$, the solution of (4) or (5), may be obtained by backpropagation along these rays to the aperture plane $z = 0$. Unfortunately, beam waves associated with the parabolic approximation cannot be represented, in general, by geometrical optics fields in the entire $z > 0$ half-space. Therefore, to successfully inverting (5), the set $\mathbf{r_o}$ should be significantly reduced. In the following discussion, we select this set to be a 2-D subspace, namely, the IP at $z = z_o$. A further reduction into a 1-D subspace has been recently addressed [22].

III. Synthesis

A. Inversion of (5)—The Synthesis Scheme

At a single frequency $\omega = \omega_0$, $\mathbf{e_t}(\mathbf{r'}, \omega_0)$ may be found by spatial inversion of the propagation operator LHS of (5) using classical time-harmonic aperture synthesis methods [11]. Thus, it is assumed throughout the paper that $\mathbf{e_t}(\mathbf{r'}, \omega_0)$ is known.

Next, we obtain $\mathbf{e_t}(\mathbf{r'}, \omega)$ for $\omega \neq \omega_0$ and $z = z_o$ through an analytic inversion of (5). Rewriting (5) for $\omega = \omega_0$

$$\frac{\omega_0}{2\pi i c z_o}\int \mathbf{dr'}\, \mathbf{e_t}(\mathbf{r'}, \omega_0) \exp\left[i\frac{\omega_0}{c}\left(\frac{r'^2}{2z_o} - \frac{\mathbf{r_o}\cdot\mathbf{r'}}{z_o}\right)\right] = \mathbf{E_t}(\mathbf{r_o}, \omega_0) \exp[-i\omega_0\tau_p(\mathbf{r_o})] \tag{8}$$

then, introducing a change of variables (scaling) $\mathbf{r'} = \mathbf{r''}\,\omega/\omega_0$, and $\mathbf{dr''} \triangleq dx''dy'' = (\omega_0/\omega)^2\,\mathbf{dr'}$, we obtain

$$\frac{\omega^2/\omega_0}{2\pi i c z_o}\int \mathbf{dr''}\mathbf{e_t}\left(\mathbf{r''}\frac{\omega}{\omega_0}, \omega_0\right) \exp\left[i\frac{\omega}{c}\left(\frac{r''^2}{2z_o}\frac{\omega}{\omega_0} - \frac{\mathbf{r_o}\cdot\mathbf{r''}}{z_o}\right)\right] = \mathbf{E_t}(\mathbf{r_o}, \omega_0)\exp[-i\omega_0\tau_p(\mathbf{r_o})]. \tag{9}$$

Finally, noting that both LHS's of (5) and (9) must be equal and utilizing the uniqueness of the Fourier transform, the result is

$$\mathbf{e_t}(\mathbf{r'}, \omega) = \frac{\omega}{\omega_0}\mathbf{e_t}\left(\mathbf{r'}\frac{\omega}{\omega_0}, \omega_0\right) \exp\left[i\frac{\omega}{c}\frac{r'^2}{2z_o}\left(\frac{\omega}{\omega_0} - 1\right)\right]. \tag{10}$$

The closed form and explicit expression given in (10) establishes the main result of this paper. The SFD $\mathbf{e_t}(\mathbf{r'}, \omega)$ is expressed in terms of the time-harmonic SFD $\mathbf{e_t}(\mathbf{r'}, \omega_0)$, indicating an appropriate ST coupling between spatial variables and temporal frequency. Equation (10), which can be considered as an ST filter at the source plane, consists of three frequency-dependent operations: gain, scaling, and focusing. The first two terms agree with the Fourier scaling rule, assuring same field energy for each frequency component, i.e., for $\omega > \omega_0$, $\mathbf{e_t}(\mathbf{r'}, \omega_0)$ is compressed while its amplitude is increased by the same ratio. The focusing term, which has a ST quadratic phase term, is inversely proportional to the IP location z_o.

Consequently, the BB field may be obtained by substituting (10) into (5), with $\mathbf{r_o} \rightarrow \mathbf{r}$

$$\mathbf{E_t}(\mathbf{r}, \omega) = \frac{\omega^2/\omega_0}{2\pi i c z} \exp[i\omega\tau_p(\mathbf{r})]\int \mathbf{dr'}\, \mathbf{e_t}\left(\mathbf{r'}\frac{\omega}{\omega_0}, \omega_0\right) \cdot \exp\left[i\frac{\omega}{c}\left(\frac{r'^2}{2z_o}\frac{\omega}{\omega_0}q - \frac{\mathbf{r}\cdot\mathbf{r'}}{z}\right)\right]$$
$$q \triangleq 1 + \frac{\omega_0}{\omega}\left(\frac{z_o}{z} - 1\right) \tag{11}$$

where $\tau_p(\mathbf{r})$ is given in (6). The time-domain BB field can be determined via inverse Fourier transformation of (11). The integral representation (11) has a form of Fresnel integral, and is valid in the paraxial region, which extends from the near-field zone to the far-field zone [15]–[20]. It can be readily shown that (11) is reduced into (3) at the IP by substituting $z = z_o$ and following a reverse of the sequence given in (8) and (9). Thus, the time envelope of the BB at the IP is similar to $s(t)$ except for a propagation delay factor $\tau_p(\mathbf{r_o})$ and a constant attenuation factor $\mathbf{E_t}(\mathbf{r_o}, \omega_0)$.

The *spatial localization* around the propagation axis can be determined by an appropriate selection of the spatial distribution $\mathbf{E_t}(\mathbf{r_o}, \omega_0)$ at $z = z_o$ via the well-known time-harmonic spatial filtering techniques [11]. Consequently, we obtain an extensive class of BB solutions since each form of a typical SFD in (10) (e.g., rectangular, circular, etc.) generates a distinct type of BB in terms of the widely tabulated Fresnel integrals in (11).

The IP *location* can be adjusted continuously from the near-field zone to the far-field zone by properly setting z_o in the focusing term in (10). As it approaches the far zone $z_o \to \infty$, the focusing term becomes negligible and (10) is reduced into

$$\mathbf{e_t}(\mathbf{r}', \omega) \sim \frac{\omega}{\omega_0}\mathbf{e_t}\left(\mathbf{r}'\frac{\omega}{\omega_0}, \omega_0\right),\ z_o \to \infty. \tag{12}$$

The remaining two operations—scaling and amplitude variation—are sufficient to obtain the frequency-independent far-zone field. Equation (12) represents a necessary and sufficient constraint that guarantees a *far-field* BB. This expression could be obtained directly via a direct inversion of the far-field version of (5), where the Fresnel integral is reduced into the Fraunhofer diffraction integral (spatial Fourier transformation of the SFD) [21]. Similarly, the BB field representation in (11) is reduced in the far-field limit into

$$\mathbf{E_t}(\mathbf{r}, \omega) \sim \frac{\omega^2/\omega_0}{2\pi i c z}\exp[i\omega\tau_f(\mathbf{r})]\int \mathbf{dr}'\,\mathbf{e_t}\left(\mathbf{r}'\frac{\omega}{\omega_0}, \omega_0\right) \cdot \exp\left[-i\frac{\omega}{c}\frac{\mathbf{r}\cdot\mathbf{r}'}{z}\right],\ z \to \infty \tag{13}$$

where $\tau_f(\mathbf{r}) \triangleq z/c$.

B. Implementation

Implementation of (10) is essential for the realization of BB. Here, we briefly discuss two alternatives: a dispersive thin lens and array-elements discretization.

1) Dispersive Thin Lens: Comparing the focusing term in (10) and the expression for a focal length f of a thin lens [21]

$$\frac{1}{f} = \left(\frac{1}{R_1} + \frac{1}{R_2}\right)(n-1) \tag{14}$$

with curvature radii R_1, R_2, and refraction index n, we obtain the following relations:

$$\frac{1}{z_o} = \left(\frac{1}{R_1} + \frac{1}{R_2}\right), \qquad n = \frac{\omega}{\omega_0} \tag{15}$$

which are essential for focusing. Here, the IP location is shifted by adjusting the curvature radii R_1, R_2, while the thin lens index of refraction varies linearly over a broad-band of frequencies.

2) Array Elements Driven by Frequency-Dependent Array Filters: Through spatial sampling of the continuous ST SFD (10), the frequency characteristics of the filter adjoined to each element are determined. Each filter is characterized as a low-pass filter prototype with a ST quadratic phase. The frequency band of each filter is inversely proportional to its distance from the array center.

IV. BB Generation via Elementary SFD's

We focus here on two opposing simple examples: Gaussian and rectangular BB SFD's. Without loss of generality, it is assumed through the next two sections that the aperture SFD is separable, thus reducing and simplifying the 3-D analysis into a 2-D scalar case, i.e., (10) and (11), are readily reduced for y-independent apertures into

$$e_t(x', \omega) = \sqrt{\frac{\omega}{\omega_0}}e_t\left(x'\frac{\omega}{\omega_0}, \omega_0\right)\exp\left[i\frac{\omega}{c}\frac{x'^2}{2z_o}\left(\frac{\omega}{\omega_0} - 1\right)\right] \tag{16}$$

$$E_t(\mathbf{r}, \omega) = \sqrt{\frac{\omega}{2\pi i c z}}\sqrt{\frac{\omega}{\omega_0}}\exp[i\omega\tau_p(\mathbf{r})]\int dx'\,e_t\left(x'\frac{\omega}{\omega_0}, \omega_0\right) \cdot \exp\left[i\frac{\omega}{c}\left(\frac{x'^2}{2z_o}\frac{\omega}{\omega_0}q - \frac{xx'}{z}\right)\right] \tag{17}$$

respectively. We derive closed-form expressions for the synthesized aperture SFD (16), and the generated BB field (17). Numerical results, highlighting the effectiveness and simplicity of our method and comparisons to other ST beams, are presented in the next section.

A. The Gaussian SFD

The Gaussian SFD given at $\omega = \omega_0$

$$e_t(x, \omega_0) = g_{a_0}(x, \omega_0) \triangleq \exp\left(-\frac{\omega_0 x^2}{2ca_0}\right) \tag{18}$$

generates via (16) and (17) the frequency-dependent SFD, and the broad-band Gaussian beam (BGB) field, respectively

$$e_t(x, \omega) = \sqrt{\frac{\omega}{\omega_0}}g_{a'}(x, \omega) \tag{19}$$

$$E_t(\mathbf{r}, \omega) = \sqrt{\frac{-ia'}{z - ia'}\frac{\omega}{\omega_0}}\exp\left(i\frac{\omega}{c}z + i\frac{\omega}{c}\frac{x^2/2}{z - ia'}\right) \tag{20}$$

where

$$a' \triangleq a_0\frac{\omega_0}{\omega}\left[1 - \frac{ia_0}{z_o}\left(1 - \frac{\omega_0}{\omega}\right)\right]^{-1}. \tag{21}$$

The BGB has the well-known form of the time-harmonic Gaussian beam [23] with an explicit expression for the frequency-dependent complex-source-point a' given in (21). It can be readily observed that the complex shift has frequency-dependent real and imaginary parts, which represent

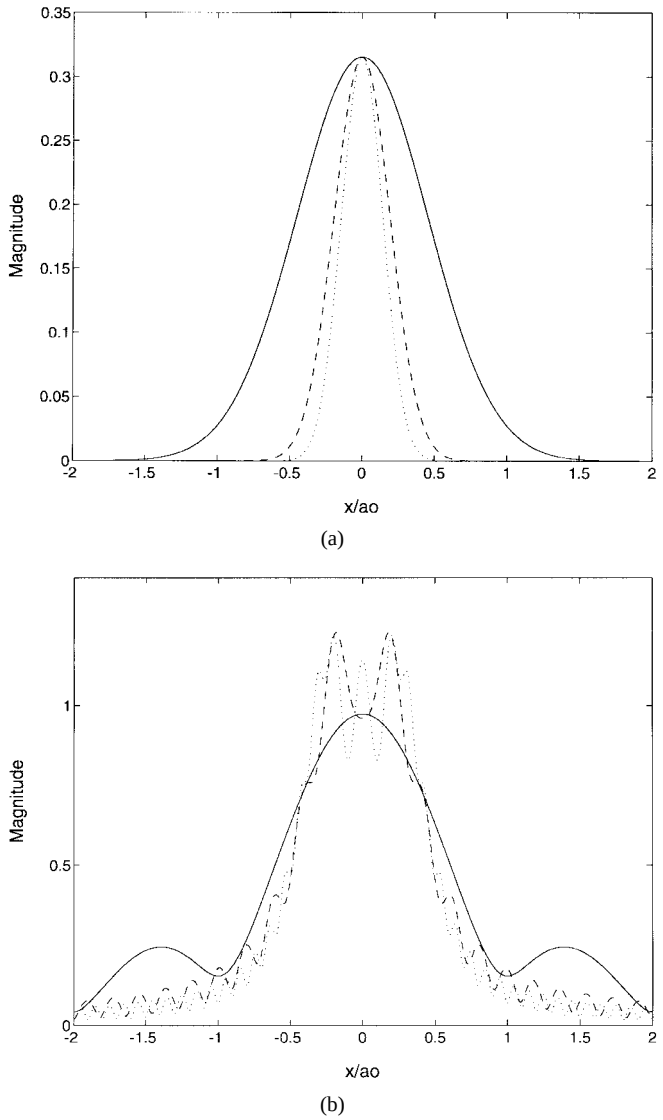

Fig. 1. Amplitude versus transverse distance x/a_0 of the (a) PGF (31) and (b) the PSF (32) at three frequencies: $\omega_{\min}$ (solid line), ω_0 (dashed line), and $\omega_{\max}$ (dotted line), $\omega_{\max}/\omega_{\min} = 10$. Low-pass filtering can be perceived for off-axis observation points, which yields smoothing of the time signal.

real (beam-waist width) and imaginary (waist location) displacements along the z axis. The constant a_0 represents the complex-source-point location of the classical time-harmonic Gaussian beam at $\omega = \omega_0$.

B. The Rectangular SFD

Here, the finite support SFD of width a_0

$$e_t(x, \omega_0) = P_{a_0}(x) \triangleq \begin{cases} 1, & \text{for } |x| \le a_0/2 \\ 0, & \text{for } |x| > a_0/2 \end{cases} \tag{22}$$

generates via (16) and (17) the frequency-dependent SFD, and the broad-band sinc-beam (BSB), respectively

$$e_t(x, \omega) = \sqrt{\frac{\omega}{\omega_0}} P_a(x) \exp\left[i\alpha_0 \frac{\omega}{\omega_0}\left(\frac{\omega}{\omega_0} - 1\right)\left(\frac{x}{a_0}\right)^2 \right] \tag{23}$$

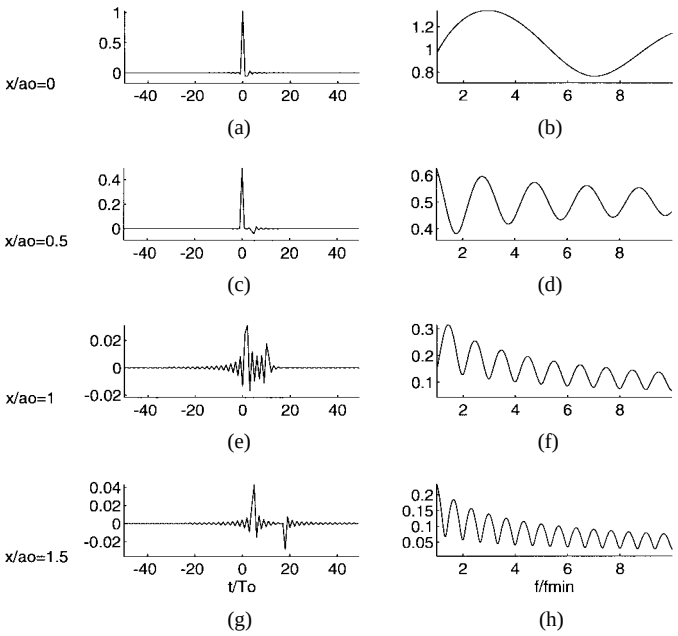

Fig. 2. The amplitude of the PSF (32) is depicted in the temporal and spectral domains at $z_o/a_0 = 10$. The time envelope of the PSF is shown in (a), (c), (e) and (g), while the signal spectrum is depicted in (b), (d), (f) and (h) at $x/a_0 = 0, 0.5, 1.0,$ and 1.5, respectively. The distortions in the time envelope, associated with additional pulses and oversmoothing of the transmitted signal, is due to periodicity and low-pass filtering in the spectral domain.

$$E_t(\mathbf{r}, \omega) = [2iqz/z_o]^{-1/2} \exp\left[i\frac{\omega}{c}\tilde{r} - i\frac{\alpha_0}{q}\left(\frac{x/a_0}{z/z_o}\right)^2 \right] \cdot [F(\nu_H) + F(\nu_L)] \tag{24}$$

where

$$a \triangleq a_0\omega_0/\omega, \quad \alpha_0 \triangleq \omega_0 a_0^2/2cz_o \tag{25}$$

$\tilde{r}$ and q are defined as in (7) and (11), respectively. The function $F(\nu)$ in (24) represents the Fresnel integral [24]

$$F(\nu) \triangleq \sqrt{2/\pi} \int_0^{\nu} dx' \exp(ix'^2) \tag{26}$$

with the following parameters:

$$\nu_L \triangleq \sqrt{\alpha_0 q}\left(\frac{1}{2} + \frac{x/a_0}{qz/z_o}\right), \quad \nu_H \triangleq \sqrt{\alpha_0 q}\left(\frac{1}{2} - \frac{x/a_0}{qz/z_o}\right). \tag{27}$$

C. Reference SFD's

For comparison purpose, we derive here reference Gaussian and rectangular SFD's, with frequency-independent width parameters, a' and a, respectively. We note that the generated reference beam fields do not support nondispersive time envelope at the IP, since their SFD's are not constructed in accordance with the proposed synthesis scheme, given in (10), or its 2-D version (16). Fixing the width parameters for all frequencies

$$a' = a = a_0 \tag{28}$$

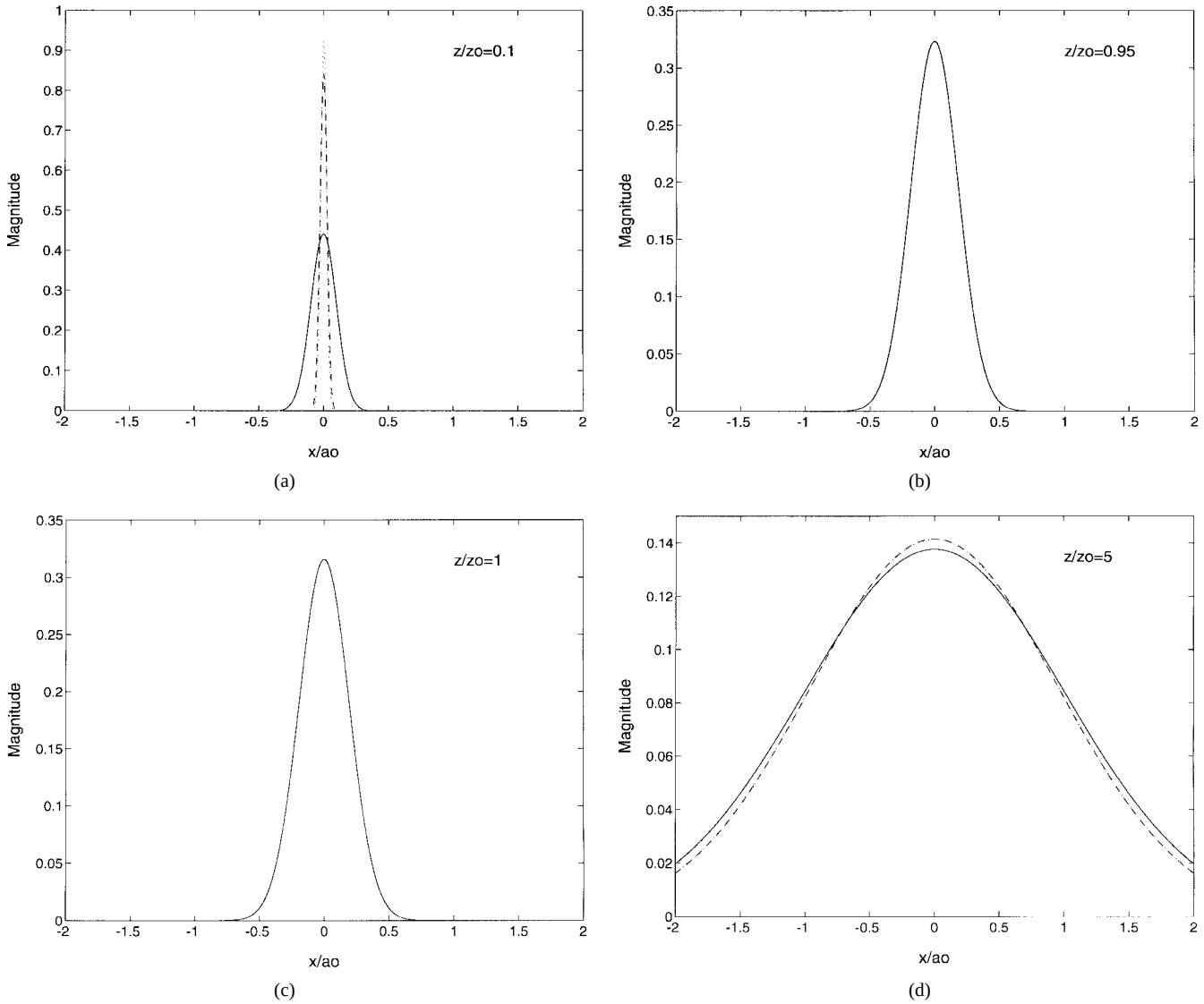

Fig. 3. Amplitude of the BGB (20) versus transverse distance x/a_0 at (a) $z/z_o = 0.1$, (b) $z/z_o = 0.95$, (c) $z = z_o$, and (d) $z/z_o = 5$, at three frequencies: $\omega_{\min}$ (solid line), ω_0 (dashed line), and $\omega_{\max}$ (dotted line). At the IP $z = z_o$ the amplitude is frequency-independent and nondispersive signal transmission can be implemented. Note the ST localization property at the proximity of this plane in (b) $z/z_o = 0.95$.

the reference SFD's

$$e_t(x, \omega) = g_{a_0}(x, \omega) \tag{29}$$

and

$$e_t(x, \omega) = P_{a_0}(x) \tag{30}$$

generate the following well-known beam fields [15], [23]: the pulsed-Gaussian-field (PGF)

$$E_t(\mathbf{r}, \omega) = \sqrt{\frac{-ia_0}{z - ia_0}} \exp\left(i\frac{\omega}{c}z + i\frac{\omega}{c}\frac{x^2/2}{z - ia_0}\right) \tag{31}$$

and the pulsed-sinc-field (PSF)

$$E_t(\mathbf{r}, \omega) = [2i]^{-1/2} \exp(i\omega z/c)\,[F(\nu_H) + F(\nu_L)]$$
$$\nu_L \triangleq \sqrt{\frac{\omega}{2cz}}\left(\frac{a_0}{2} + x\right), \quad \nu_H \triangleq \sqrt{\frac{\omega}{2cz}}\left(\frac{a_0}{2} - x\right) \tag{32}$$

respectively.

V. Simulation Results

A. The Signal

The signal spectrum $s(\omega)$ given in (1), is selected to be constant over the frequency band

$$s(\omega) = \begin{cases} 1, & \text{for } |\omega| \epsilon [\omega_{\min}, \omega_{\max}] \\ 0, & \text{otherwise} \end{cases} \tag{33}$$

to avoid any impact of the signal spectrum upon the BB or the reference pulsed fields. Thereby, focusing only on the dispersive characteristics of the propagation mechanism. To maintain the paraxial approximation in the space coordinates the effective aperture length $L(\omega)$ contains at least ten wavelengths in the entire frequency band

$$\frac{L(\omega)\omega}{2\pi c} \geq 10, \quad \omega > 0. \tag{34}$$

The frequency ω_0 is taken to be $\omega_0 = (\omega_{\min} + \omega_{\max})/2$ and chosen as the carrier frequency of the base-band signal, which

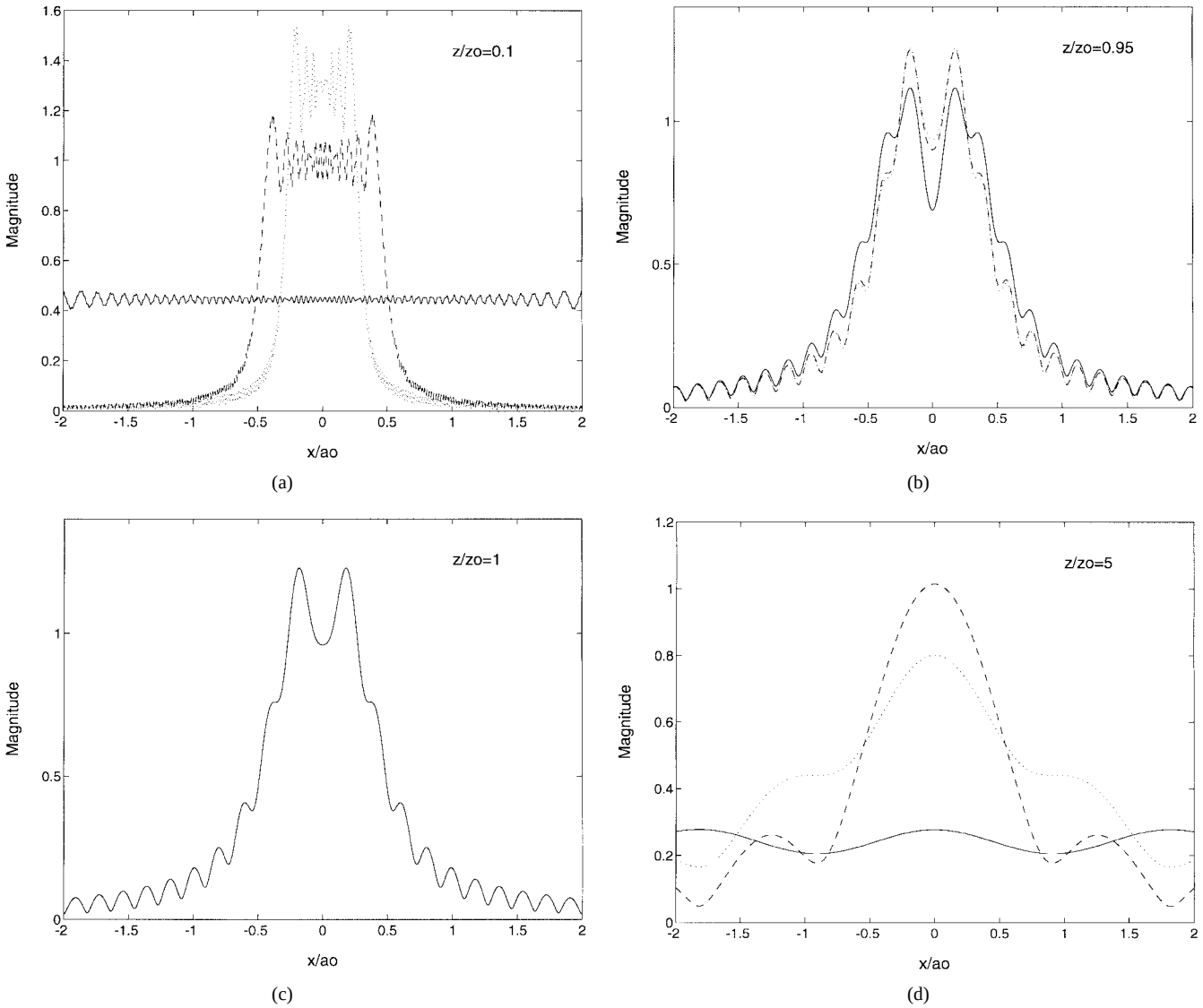

Fig. 4. Same as Fig. 3 but for the BSB (24).

has an information bandwidth $W \triangleq (\omega_{\max} - \omega_{\min})/2\pi$ with $T_0 \triangleq 1/W$.

B. The Reference Pulsed Field: PGF and PSF

In the narrow-band limit ($\omega_{\max}/\omega_{\min} \approx 1$) all the time-harmonic beam constituents in the frequency band have approximately the same amplitude distribution. Consequently, the spectral content of the pulsed field at a given plane is nearly constant and no significant signal dispersion is expected. However, in the broad-band limit $\omega_{\max}/\omega_{\min} \gg 1$ we expect that the proposed synthesis scheme reduces significantly the signal dispersion and, thus, select throughout this section $\omega_{\max}/\omega_{\min} = 10$. For this bandwidth ratio, as shown in Fig. 1(a) and (b), for the PGF and PSF, respectively, the amplitude distributions have strong deviations and low-pass filtering at off-axis points can be observed. Notice that the two SFD's (29) and (30) are inherently different. The PGF SFD width depends on the frequency, while the PSF SFD is constant over the entire bandwidth. This property explains the stronger low-pass filter decaying in the Gaussian case, in which the effective aperture width decreases as the frequency increases.

An interesting property of the PGF (31) is the nondispersive transmission of signal to each on-axis point $x = 0$ but not to off-axis points, i.e., along a real ray, also known as the central ray [17], which is in agreement with the discussion at the end of Section II and in [22]. Yet, for the rectangular SFD where no real ray exists, distortions occur along the z axis as well, as shown in Fig. 2(a). The signal distortions shown in Fig. 2(a), (c), (e), and (g), associated with additional pulses and over smoothing of the transmitted pulse are due to periodicity and low-pass filtering, as depicted in Fig. 2(b), (d), (f), and (h) for $x/a_0 = 0, 0.5, 1.0$, and 1.5, respectively. Also note that the time interval between the pulses is related to the transverse distance from the off-axis point to the beam axis.

C. The BB Field: BGB and BSB

The characteristics and effectiveness of the proposed synthesis method are demonstrated for the BGB and the BSB.

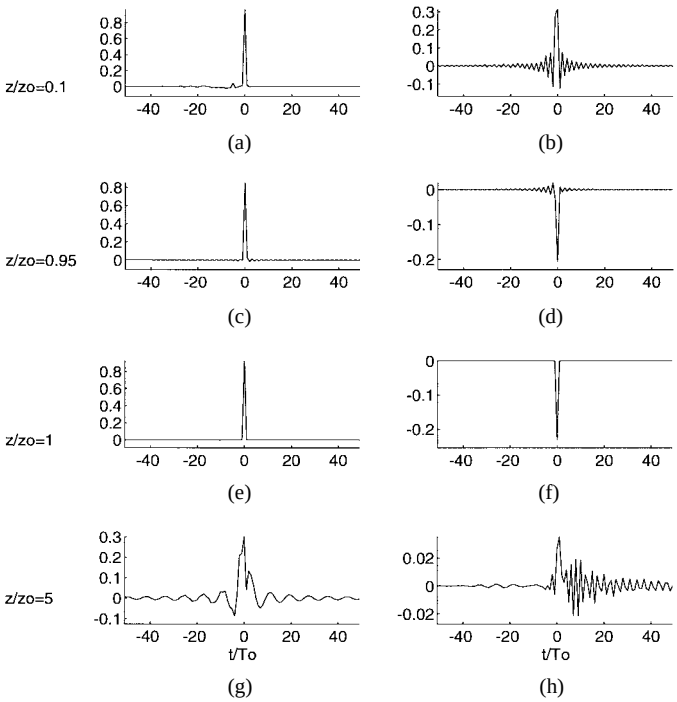

Fig. 5. The amplitude of the BSB (24) is shown for on-axis $x = 0$ and off-axis $x/a_0 = 0.8z/z_o$ observation points, at the same plane location as in Fig. 4. At the IP the time envelope is identical with the predetermined broad-band $\omega_{\max}/\omega_{\min} = 10$ transmitted time signal.

The amplitude of the BGB (20) and the BSB (24) is depicted in Figs. 3 and 4, respectively, for several planes perpendicular to the beam-axis: 1) $z/z_o = 0.1$; 2) $z/z_o = 0.95$; 3) $z = z_o$; and 4) $z/z_o = 5$ at three frequencies: $\omega_{\min}, \omega_0$, and $\omega_{\max}$. The IP is taken to be in the near-field zone $z_o/a_0 = 10$ of the time-harmonic beam at $\omega = \omega_0$. At the IP, the BGB and the BSB amplitude distribution coincide, for all frequencies with the amplitude distribution of the time-harmonic Gaussian and sinc-beam at $\omega = \omega_0$, respectively. Since the phase at this plane is linear in frequency, the signal is transmitted without distortions.

The time envelope of the BSB is depicted, in Fig. 5 for on-axis $x = 0$ and off-axis $x/a_0 = 0.8z/z_o$ observation points at the same plane locations as in Fig. 4. Notice, from Fig. 5(a) and (b) at $z/z_o = 0.1$ for on-axis and off-axis points, respectively, that the signal emerges at earlier time from off-axis points at the source plane and it has different time variations than the on-axis signal. While there are still distortions in the time envelope near the IP at $z/z_o = 0.95$, as shown in Fig. 5(c) and (d) for $x = 0$ and $x/a_0 = 0.76$, respectively, the distortions disappear at the IP, as shown in Fig. 5(e) and (f) for $x = 0$ and $x/a_0 = 0.8$, respectively. Also note that the off-axis point is outside the effective beam width at that plane. However, far from the IP at $z/z_o = 5$ the time envelope of the BSB undergoes dispersion for both on-axis and off-axis points, as shown in Fig. 5(g) and (h), respectively.

VI. Summary and Conclusions

This paper deals with ST aperture synthesis for the generation of prescribed broad-band time signal at a given plane. The synthesis is performed within the framework of the parabolic approximation (Fresnel integral) in the spatial variables, applicable for radiation fields localized around the propagation axis.

The ST SFD solution for the aperture synthesis problem is unique and presented in a closed-form explicit expression in (10). The solution, the main result of this paper, is formulated in terms of a time-harmonic SFD at $\omega = \omega_0$, which undergoes frequency-dependent focusing, scaling, and amplitude variations that are not dependent on the signal spectrum, but rather on its frequency band. Thus, each time-harmonic SFD defines via (10) a distinct BB field solution, which supports a predetermined time envelope at the IP. The location of this plane can be varied continuously from the near-field zone to the far-field zone by changing the z_o parameter in the focusing term.

Although the nondispersive time signal is obtained at a single plane it is localized in ST at the proximity of this plane as well. Thus, in that region the BB is reduced into a pulsed beam, which maintains its analytical ST structure along the propagation axis. However, since this location can be arbitrarily determined it is possible to convey localized field with predetermined ST structure to any region in the near-field or far-field zones.

Sensitivity analysis for the proposed synthesis scheme has been carried out in [8]. It is demonstrated that, in general, the BB field solutions for the BGB as well as for the BSB are stable, i.e., small variations in the SFD parameters: gain, scaling, and focusing, cause small variations in the BB field at the IP, even in the near-field zone.

References

[1] R. W. Ziolkowski, "Properties of electromagnetic beams generated by ultra-wide bandwidth pulse-driven arrays," *IEEE Trans. Antennas Propagat.*, vol. 40, pp. 888–905, Aug. 1992.

[2] A. M. Shaarawi, I. M. Besieris, R. W. Ziolkowski, and S. M. Sedky, "Generation of approximate focus-wave-mode pulses from wide-band dynamic Gaussian apertures," *J. Opt. Soc. Amer. A*, vol. 12, pp. 1954–1964, 1995.

[3] P. D. Einziger and S. Raz, "Wave solutions under complex space-time shifts," *J. Opt. Soc. Amer. A*, vol. 4, pp. 3–10, 1987.

[4] E. Heyman and L. B. Felsen, "Complex-source pulsed-beam fields," *J. Opt. Soc. Amer. A*, vol. 6, pp. 806–817, 1989.

[5] Y.-W. Kang and D. M. Pozar, "Optimization of pulse radiation from dipole arrays for maximum energy in a specified time interval," *IEEE Trans. Antennas Propagat.*, vol. AP-34, pp. 1383–1390, Dec. 1986.

[6] D. M. Pozar, Y.-W. Kang, and D. H. Schaubert, "Optimization of the transient radiation from dipole array," *IEEE Trans. Antennas Propagat.*, vol. AP-33, pp. 69–75, Jan. 1985.

[7] J. E. Hernandez, R. W. Ziolkowski, and S. R. Parker, "Synthesis of the driving functions of an array for propagating localized wave energy," *J. Acoust. Soc. Amer.*, vol. 92, no. 1, pp. 550–562, July 1992.

[8] I. Dvir, "On the propagation of waves and beams in linear and nonlinear media," Ph.D. dissertation, Technion, Israel, 1994 (in Hebrew).

[9] I. Dvir and P. D. Einziger, "On the transmission of an undistorted broadband pulsed-beam," in *URSI Radio Sci. Meet.*, Ann Arbor, MI, 1993, p. 357.

[10] ——, "Transmission of an undistorted broadband pulsed-sinc-beam," *Ultra-Wideband Short-Pulse Electromagnetics 2*, L. Carrin and L. B. Felsen, Eds. New York: Plenum, 1995, pp. 365–370.

[11] R. S. Elliot, *Antenna Theory and Design.* Englewood Cliffs, NJ: Prentice-Hall, 1981.

[12] D. L. Sengupta and C.-T. Tai, "Radiation and reception of transients by linear antennas," in *Transient Electromagnetic Fields—Volume 10, Topic in Applied Physics*, L. B. Felsen, Ed. New York: Springer-Verlag, 1976, ch. 4, pp. 182–234.

[13] P. C. Clemmow, *The Plane Wave Spectrum Representation of Electromagnetic Fields.* New York: Pergamon, 1966.

[14] P. D. Einziger, S. Raz, and M. Shapira, "Gabor representation and aperture theory," *J. Opt. Soc. Amer. A*, vol. 3, no. 4, pp. 508–522, 1986.
[15] J. Goodman, *Introduction to Fourier Optics*, 2nd ed. New York: McGraw-Hill, 1996.
[16] J. A. Arnaud, *Beam and Fiber Optics.* New York: Academic, 1976.
[17] V. M. Babic and N. Y. Kirpicnikova, *The Boundary-Layer Method in Diffraction Problems.* New York: Springer-Verlag, 1979.
[18] H. A. Haus, *Waves and Fields in Optoelectronics.* Englewood Cliffs, NJ: Prentice-Hall, 1984.
[19] A. Siegman, *Lasers.* Mill Valley, CA: Univ. Sci., 1986.
[20] W. H. Southwell, "Validity of the Fresnel approximation in the near field," *J. Opt. Soc. Amer.*, vol. 71, no. 1, pp. 7–14, 1981.
[21] M. Born and E. Wolf, *Principles of Optics.* New York: Pergamon, 1975.
[22] I. Dvir and P. D. Einziger, "Broadband beam generation for an on-axis nondispersive time-signal propagation," *J. Opt. Soc. Amer. A*, to be published.
[23] G. A. Deschamps, "Gaussian beams as a bundle of complex rays," *Electron. Lett.*, vol. 7, no. 23, pp. 684–685, 1971.
[24] M. Abramovich and I. Stegun, *Handbook of Mathematical Function.* New York: Dover, 1970.

Itsik Dvir was born in Haifa, Israel, on January 3, 1959. He received the B.Sc., M.Sc., and Ph.D. degrees in electrical engineering from the Technion-Israel Institute of Technology, Haifa, Israel, in 1987, 1990, and 1994, respectively.

In 1994, he was with the Department of Electrical Engineering at the Technion, where he is currently an Adjunct Teaching Associate. Since November 1994 he has been with RAFAEL. His current interests are in both signal processing and electromagnetic wave theory, including broad-band beams, nonlinear wave phenomena, speech, and array signal processing.

Pinchas D. Einziger was born in Tel Aviv, Israel, on April 24, 1949. He received the B.Sc. and M.Sc. degrees in electrical engineering from the Technion-Israel Institute of Technology, Haifa, Israel, in 1976 and 1978, respectively, and the Ph.D. degree in electrophysics from the Polytechnic University, Brooklyn, NY, in 1981.

Since 1981, he has been on the faculty of the Department of Electrical Engineering at the Technion. His main interests are in electromagnetic wave theory, nonlinear wave phenomena, and bioelectromagnetics.